

Modeling the Effect of Mixed Emulsifier Systems in Emulsion Copolymerization

ELIAS UNZUETA, JACQUELINE FORCADA

Grupo de Ingeniería Química, Departamento de Química Aplicada, Facultad de Ciencias Químicas, Universidad del País Vasco/EHU, Apdo: 1072, 20080 Donostia, San Sebastián, Spain

Received 3 October 1996; accepted 24 March 1997

ABSTRACT: A mathematical model for the emulsion copolymerization of methyl methacrylate and butyl acrylate has been developed. This model, which applies the method of moments of a distribution to model the evolution of the particle size distribution, predicts the effects of the concentration and composition of anionic/nonionic surfactant systems on the polymerization process and on the characteristics of the product obtained, including particle nucleation, growth, and coagulation. Nucleation is a dynamic process in which the surfactant system affects the competition between homogeneous and heterogeneous nucleation, with simultaneous coagulative processes of precursor particles. The effect of the surfactant system on nucleation is described mathematically using a variable radical critical chain length, j_{cr} . The solution properties of surfactant mixtures, mainly critical micelle concentration and micelle composition, were predicted using the thermodynamics of nonideal mixtures. A good agreement between model predictions in batch and semicontinuous reactors and experimental results was found. © 1997 John Wiley & Sons, Inc. *J Appl Polym Sci* **66**: 445–458, 1997

Key words: emulsion copolymerization; mathematical modeling; particle size distribution; surfactant system; nucleation

INTRODUCTION

Mathematical modeling of emulsion polymerization has received much attention in recent years. The long-range goal of modeling is prediction¹ and, better, the obtention of the optimum process to achieve the desired product by previously specifying its characteristics. However, current knowledge of emulsion polymerization permits only a limited understanding of the mechanisms involved by fitting experimental data in a determinate polymerization system.

Since the first models explaining the mechanism of emulsion polymerization developed by Harkins² and Smith and Ewart,³ from models predicting the polymerization rate,⁴ properties of the polymer obtained^{5,6} (molecular weight and copolymer composition), and colloidal characteristics⁷ (particle number and particle size distributions); to models applied to optimum process design and control,^{8–11} a great effort has been made in the theoretical background of emulsion polymerization.

The particle nucleation is the main and most difficult process to model, and determines the subsequent evolution of the reaction and the quality of the latex. Nowadays, it is assumed that particle nucleation is a dynamic process, in which formation and stabilization of latex particles occurs whether in the continuous phase, in micelles, and/or in monomer droplets. HUFT theory^{12,13} is the

Correspondence to: J. Forcada.

Contract grant sponsor: Comision Interministerial de Ciencia y Tecnología; contract grant number: MAT96-1035-C03-01.

Contract grant sponsor: Gipuzkoako Foru Aldundia.

Journal of Applied Polymer Science, Vol. 66, 445–458, 1997
© 1997 John Wiley & Sons, Inc. CCC 0021-8995/97/030445-14

mathematical description of nucleation in these loci that best fits most experimental data.

The mathematical model developed in this work takes well-defined mathematical descriptions of several processes from previous models. The comonomer consumption and its concentrations in the different phases, radical balances between the particle and aqueous phases, and rate constants for physicochemical processes (absorption, desorption, and gel effect) were taken from the references indicated in the text.

On the other hand, the innovative effort of this model was directed:

- To stress the effect of mixed surfactant systems (anionic/nonionic) in emulsion polymerization and, mainly, in the nucleation stage.
- To unify criteria for the nucleation process, based on HUFT and coagulative nucleation theories, with a comprehensive picture in which the emulsifier system affects the growth of oligoradicals in the aqueous phase.
- To model the evolution of the particle size distribution, including particle nucleation, growth, and coagulation.

The method of moments of a distribution was used to model the evolution of the particle size distribution.

EXPERIMENTAL

The experimental results used to check the model predictions and to adjust several parameters have been described in earlier works.^{14,15} Those papers describe the results obtained in the study of the effect of mixed surfactant systems in the emulsion copolymerization of methyl methacrylate (MMA) and butyl acrylate (BuA) in a semicontinuous reactor. Seeded and nonseeded reactions were carried out, and anionic and nonionic emulsifiers were used. The effect of the emulsifier concentration and emulsifier system composition was studied, covering a wide range of concentrations [above and below the critical micelle concentration (*cmc*)].

The anionic emulsifier was sodium lauryl sulfate (SLS) and the non-ionic one was polyethylene oxide lauryl ether (Brij35).

MODEL DESCRIPTION

In this model a deterministic approach is made, so the overall particle balance is used with no distinction between particles with different numbers of radicals. In this way, the particle growth rate is defined by the average radical number per particle for the overall particle population.

The particle population balance includes the particle size distribution (PSD). This leads to a mathematical system composed by ordinary and partial differential equations. To solve this, an ordinary differential equation system is obtained using the method of moments of a distribution. The k th order moment of a particle size distribution, referred to radius, is defined as

$$\mu^k = \int_0^\infty n(r)r^k dr \quad (1)$$

where, $n(r)$ is the probability function of the particles of radius r .

Using combinations of the moments of the PSD, the following average particle sizes can be obtained:

$$\bar{d}_n = 2 \times \frac{\mu^1}{\mu^0} \quad (2)$$

$$\bar{d}_w = 2 \times \frac{\mu^4}{\mu^3} \quad (3)$$

$$\bar{d}_v = 2 \times \left(\frac{\mu^3}{\mu^0} \right)^{1/3} \quad (4)$$

$$\bar{d}_a = 2 \times \left(\frac{\mu^2}{\mu^0} \right)^{1/2} \quad (5)$$

where, \bar{d}_n , \bar{d}_w , \bar{d}_v , and \bar{d}_a , are the number, weight, volume, and area average particle diameters, respectively.

The ordinary differential equation system described below was solved by numerical integration using the Gear¹⁶ method.

The mathematical method used to obtain the PSD from its moments is based on the expansion of Hermite polynomials, a method previously applied to emulsion polymerization by Min.¹⁷

Material Balances

The material balances of comonomers include monomer consumption both in particles and in

the aqueous phase and the respective feed terms. In this work, methyl methacrylate is referred as A and butyl acrylate as B.

$$\frac{dA}{dt} = -(k_{pAA}P_A^p + k_{pBA}P_B^p)[A]_p \frac{\bar{n}N_p}{N_A} - (k_{pAA}P_A^w + k_{pBA}P_B^w)[A]_w R_w \frac{V_w}{\Phi_w^{aq}} + F_A \quad (6)$$

$$\frac{dB}{dt} = -(k_{pBB}P_B^p + k_{pAB}P_A^p)[B]_p \frac{\bar{n}N_p}{N_A} - (k_{pBB}P_B^w + k_{pAB}P_A^w)[B]_w R_w \frac{V_w}{\Phi_w^{aq}} + F_B \quad (7)$$

where k_{pij} is the polymerization rate constant between radical i and monomer j ; $[i]_j$, the concentration of monomer i in phase j ; \bar{n} , the average radical number per particle; N_p , the total particle number; N_A , Avogadro's constant; R_w , the radical concentration in the aqueous phase; ϕ_w^{aq} , the volumetric fraction of water in the aqueous phase; and F_i , the feed rate of monomer i . P_i^j is defined¹⁸ as the probability of a growing chain in phase j having the growing radical on the i monomeric unit:

$$P_A^j = \frac{k_{pBA}[A]_j}{k_{pBA}[A]_j + k_{pAB}[B]_j} \quad (8)$$

$$P_B^j = 1 - P_A^j \quad (9)$$

Monomer concentrations in the aqueous phase, monomer droplets, and polymer particles were obtained using the partition constants method.^{19,20}

The balance of the volume of water (V_w) is defined as

$$\frac{dV_w}{dt} = Q_w \quad (10)$$

where Q_w is the volumetric water feeding rate.

The material balance of initiator includes feed and consumption by decomposition:

$$\frac{dI}{dt} = -k_I I + F_I \quad (11)$$

where k_I is the decomposition rate of initiator; I , the initiator amount; and F_I , the initiator molar feed rate.

The material balance for the emulsifier i is written as

$$\frac{dE_i}{dt} = F_{E_i} \quad (12)$$

where F_{E_i} is the feed rate of emulsifier i .

Population Balances

The theoretical scope for nucleation used in this work assumes a coagulative nucleation mechanism, hence two particle population balances are defined: the population balance for precursor particles (N^*) and the balance for mature particles (N_p).

The population balance for precursor particles is defined as

$$\frac{dN^*}{dt} = R_g - k_g^{**} \frac{(N^*)^2}{V_w} - k_g^{*p} \frac{N^* N_p}{V_w} \quad (13)$$

where k_g^{**} is the coagulation rate constant between precursor particles; k_g^{*p} , the coagulation rate constant between precursor and mature particles; N^* and N_p , the total number of precursor and mature particles, respectively; and R_g , the formation rate of precursor particles, defined below.

The population balance for the k th order moment of the PSD is defined as

$$\begin{aligned} \frac{d\mu^k}{dt} = & k\bar{n}\mu_g^{k-1} + P_N k_g^{**} \frac{(N^*)^2}{V_w} r_{po}^k \\ & + \frac{1}{2} k_g \frac{1}{V_w} \sum_{j=0}^k \binom{k}{j} \mu^{k-j} \mu^j (0.2599)^j \\ & - k_g \frac{1}{V_w} \mu^0 \mu^k \quad (14) \end{aligned}$$

where μ_g is defined below; P_N , the probability of a precursor particle to become a mature particle; r_{po} , the initial radius of particles; and k_g , the coagulation rate constant between particles. The first term of this equation refers to the volumetric growth of particles by propagation, the second is the nucleation of new particles, and the last ones are coagulation terms. The μ_g is the moment of the particle growing rate distribution, referred to the radius and defined as

$$\mu_g^k = \int_0^\infty \frac{1}{4\pi} \frac{dv_p(t)}{dt} \frac{1}{r^2} n(r) r^k dr \quad (15)$$

where v_p is the particle volume, and $n(r)$ the probability function of particles with radius r .

The population balance of mature particles is obtained by rewriting eq. (14) for the moment of order 0 ($k = 0$):

$$\frac{dN_p}{dt} = \frac{d\mu^0}{dt} = P_N k_g^{**} \frac{(N^*)^2}{V_w} + \frac{1}{2} k_g \frac{1}{V_w} \mu^0 \mu^0 \quad (16)$$

Radical Balances

Applying the pseudosteady state assumption, the average radical number per particle (\bar{n}) is obtained using the method proposed by Ugelstad and Hansen²¹:

$$\bar{n} = \frac{a^2/8}{m + \frac{a^2/4}{m + 1 + \frac{a^2/4}{m + 2 + \dots}}} \quad (17)$$

$$a = 8k_A N_A \frac{R_w}{V_w} \frac{v_p}{\bar{k}_{tp}} \quad (18)$$

$$m = k_d N_A \frac{v_p}{\bar{k}_{tp}} \quad (19)$$

where k_a and k_d are the absorption and desorption rate constants, respectively; R_w , the radical concentration in the aqueous phase; v_p , the particle volume; and \bar{k}_{tp} , the average radical termination rate constant in particles.

This equation is solved simultaneously with the radical balance in the aqueous phase:

$$R_w = \frac{-(k_{am} N_m / V_w + k_a N_p / V_w) + [(k_{am} N_m / V_w + k_a N_p / V_w)^2 + 8\bar{k}_{tw} / \Phi_w^{aq} (\rho_I + k_d \bar{n} N_p / V_w)]^{1/2}}{4\bar{k}_{tw} / \Phi_w^{aq}} \quad (20)$$

where k_a and k_{am} are the absorption rate constant into particles and micelles, respectively; N_p and N_m , the overall particle and micelle numbers, respectively; \bar{k}_{tw} , the average radical termination rate constant in aqueous phase; Φ_w^{aq} , the volumetric fraction of water in the aqueous phase; and ρ_I , the radical generation rate from initiator, defined as

$$\rho_I = 2fk_I I \quad (21)$$

where k_I is the initiator decomposition rate con-

stant; I , the initiator amount; and f , the efficiency factor.

Physicochemical Constants

Radical absorption rate constant to particles and micelles is obtained assuming the diffusional mechanism proposed by Fitch and Shih²²:

$$k_a = 4\pi D_w r_p N_A F_p \quad (22)$$

$$k_{am} = 4\pi D_w r_m N_A F_m \quad (23)$$

where r_p and r_m are the particle and micelle radii, respectively; D_w , the radical diffusion constant in the aqueous phase; and F_p and F_m , the radical absorption efficiencies.

The radical desorption rate constant is assumed to be the sum of the rate constants:

$$k_d = k_{dA} + k_{dB} \quad (24)$$

A previous radical transfer reaction to monomer²³ must take place before the radical desorption. For the radical i , the desorption rate constant is obtained as follows:

$$k_{di} = \frac{(k_{fii} P_i^p + k_{fji} P_j^p)[i]_p}{\frac{r_p^2}{2D_p} (k_{pii}[i]_p + k_{pij}[j]_p) + 1} \quad (25)$$

where k_{fij} and k_{pij} are the transfer and propagation rate constants, respectively; between the i radical and the j monomer; P_i^p , the probabilities defined above; r_p , the radius of the particle; D_p , the diffusion rate constant for radicals in the particle; and $[i]_p$, the concentration of monomer i in the particle.

The radical termination rate constant in phase i is obtained as

$$\bar{k}_{ii}^o = k_{iAA}^o (P_A^i)^2 + (k_{iAB}^o + k_{iBA}^o) P_A^i P_B^i + k_{iBB}^o (P_B^i)^2 \quad (26)$$

where k_{ij}^o is the termination rate constant between i and j radicals; and P_i^j , the probabilities defined above.

Both the transfer and termination rate constants between the comonomers are obtained as the geometric average of the rate constants for homopolymerization.

The gel effect has a great effect in polymerization kinetics.²⁴ Termination rate constant in the

particle is obtained from the termination kinetic constant affected by a gel effect parameter (g^2) as

$$\bar{k}_{tp} = \bar{k}_{tp}^o g^2 \quad (27)$$

where for copolymerization

$$g^2 = (g_A^2 g_B^2)^{1/2} \quad (28)$$

The experimental relationship between gel effect and conversion used for MMA is¹⁸

$$g_A^2 = (\exp\{-0.94x_p - 3.87x_p^2 + 0.49x_p^3\})^2 \quad (29)$$

where x_p is the conversion in the particle.

Taking into account the low termination constant for BuA, it was considered that this monomer does not lead to a significant gel effect when copolymerizing with MMA:

$$g_B^2 = 1 \quad (30)$$

Nucleation

The basis of the nucleation mechanism described in this work is the HUFT theory, where oligoradicals propagate in the aqueous phase up to their critical chain length, at which point they precipitate as precursor particles that grow mainly by coagulation but also by propagation. In this picture, surfactant molecules not only provide colloidal stability. In fact, surfactant micelles play a fundamental role as nucleation promoters. Classically, homogeneous and heterogeneous nucleation mechanisms have been considered as separate processes with one of them usually predominating. As Hansen²⁵ has pointed out, in this model it is considered that surfactant micelles increase the overall growing rate of the oligoradicals in the aqueous phase, increasing their probability both to precipitate from the aqueous phase and to nucleate a new particle from a micelle.

Mathematically, this effect has been included assuming that the effect of micelles is the reduction of the critical length (j_{cr}). In this model, j_{cr} is a function of emulsifier concentration.

In eq. (13) the precursor particle nucleation rate term (R_g) was included. Applying Hansen's theory for homogeneous nucleation,²⁶ the rate of precursor particle formation can be expressed as

$$R_g = \frac{(2fk_t I + k_d \bar{n} N_p)_{N_A}}{\left(1 + \frac{k_a N_p / V_w}{\sum k_{pi}[i]_w} + \frac{2\bar{k}_{tw} R_w}{\sum k_{pi}[i]_w}\right)^{(j_{cr}-1)} \quad (31)$$

Moreover, the propagation rate in the aqueous phase is defined as

$$\begin{aligned} \sum k_{pi}[i]_w = & (k_{pAA} P_A^w + k_{pBA} P_B^w)[A]_w \\ & + (k_{pBB} P_B^w + k_{pAB} P_A^w)[B]_w \quad (32) \end{aligned}$$

where $[i]_w$ is the concentration of monomer i in the aqueous phase; k_{pij} , the propagation rate constants between radical i and monomer j ; and P_i^w , the probabilities defined above.

The critical chain length j_{cr} of an oligoradical is related to the micelle number that is calculated by taking into account the composition and nature of the surfactant system, the critical micelle concentration of the surfactant mixture, and the adsorption isotherms of the mixed surfactant system.

To obtain the mathematical relationship between the critical length, j_{cr} , and the micelle number, N_m , it is assumed that the value of j_{cr} must equate the probability for an oligoradical in the aqueous phase to enter in a micelle to that of precipitation by propagation:

$$R_h^{(j_{cr}-1)} = R_m = 1 - R_h \quad (33)$$

where R_h and R_m are defined as

$$R_h = \frac{\sum k_{pi}[i]_w}{\sum k_{pi}[i]_w + k_{am} N_m / V_w} \quad (34)$$

where k_{am} is the radical absorption rate constant into micelles; and N_m , the overall micelle number.

From eq. (33),

$$j_{cr} = 1 + \frac{\log(1 - R_h)}{\log(R_h)} \quad (35)$$

This equation loses its physical sense when R_h approaches 1 or 0, and boundary values must be arbitrarily assumed. Thus, when R_h equals 0, pure micellar nucleation takes place and j_{cr} is fixed at 5²⁷ (mathematically, the lowest value admitted for j_{cr} is 0.075); and when R_h is 1, only homogeneous nucleation occurs and j_{cr} is assumed to be 40.¹³ With these assumptions, eq. (35) can be written as

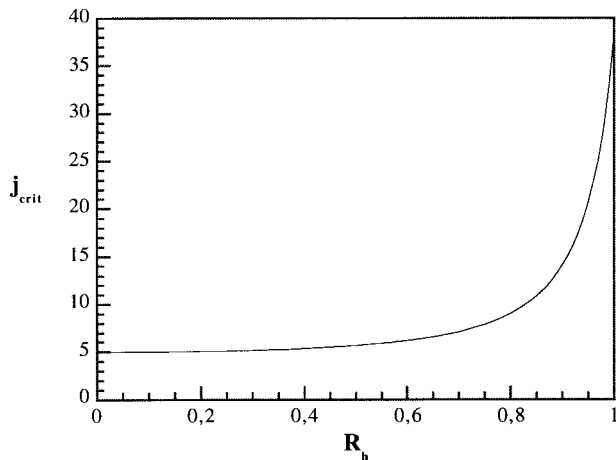


Figure 1 Variation of j_{crit} with R_h .

$$j_{cr} = 5 + \frac{\log(1.075 - R_h)}{\log(R_h - 0.075)} \quad (36)$$

Figure 1 shows the evolution of j_{cr} with R_h calculated from eq. (36).

The probability for one precursor particle to become a mature particle [P_N term in eq. (14)] is calculated as

$$P_N = K'_n \exp \left\{ -K''_n \frac{(cmcV_w - E_w)}{cmcV_w} \right\} \quad (37)$$

where K'_n and K''_n are adjustable parameters; cmc , the critical micelle concentration; and E_w , the free surfactant amount in the aqueous phase.

On the other hand, the critical radius to consider a particle as a mature particle (r_{po}) is obtained as

$$r_{po} = \frac{r_o^*}{(P_N)^{1/3}} \quad (38)$$

where r_o^* is the initial radius of precursor particles.

Partition of the Surfactant System

The modeling of the surfactant mixture is based on the thermodynamics of nonideal mixtures.²⁸

The composition of the surfactant system is defined as

$$\alpha = \frac{E_1}{E_1 + E_2} \quad (39)$$

where E_1 and E_2 are the anionic and nonionic emulsifiers, respectively.

The micelle composition is defined in the same way:

$$\alpha^m = \frac{E_1^m}{E_1^m + E_2^m} \quad (40)$$

where E_1^m and E_2^m are the amount of anionic and nonionic emulsifiers, respectively, in the micelles.

The critical micelle concentration of surfactant mixture (cmc_{12}) and the composition of micelles can be calculated using the thermodynamic theory for nonideal mixtures, using these expressions:

$$\begin{aligned} (\alpha^m)^2 \ln \left(\frac{\alpha cmc_{12}}{\alpha^m cmc_1} \right) \\ = (1 - \alpha^m)^2 \ln \left(\frac{(1 - \alpha) cmc_{12}}{(1 - \alpha^m) cmc_2} \right) \end{aligned} \quad (41)$$

$$\ln \left(\frac{\alpha cmc_{12}}{\alpha^m cmc_1} \right) = \beta^m (1 - \alpha^m)^2 \quad (42)$$

where α and α^m are the composition of the surfactant mixture and micelles, respectively; cmc_1 , cmc_2 , and cmc_{12} , the critical micelle concentrations of single (anionic and nonionic) and mixed surfactant systems; and β^m , the interaction parameter.

The nature of the surfactant mixture is defined by the interaction parameter (β^m). Negative interaction parameters mean attractive or compatible nature, positive ones indicate repulsive forces, and zero indicates no interaction between the emulsifiers. The calculation of the interaction parameter is the basis for characterizing the surfactant mixture,²⁹⁻³³ so it allows, using eqs. (41) and (42), the critical micelle concentration of the emulsifier mixture (cmc_{12}) and the composition of the micelles (α^m) at any surfactant mixture composition to be obtained theoretically.

In this work, the interaction parameter between SLS and Brij35 was obtained experimentally. Critical micelle concentrations were obtained by measuring surface tensions at different surfactant concentrations for different surfactant mixture compositions. Figure 2 shows the obtained experimental values. In this figure a very good agreement between experimental data and theoretical predictions is found when the interac-

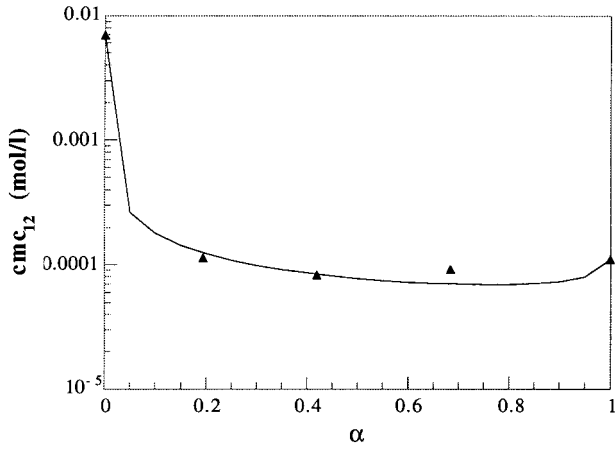


Figure 2 Critical micelle concentration of surfactant mixture versus surfactant mixture composition, assuming $\beta^m = -8$: (\blacktriangle) experimental; (—) theoretical.

tion parameter (β^m) is -8 . This value, used in the mathematical model, implies quite strong interaction between these two emulsifiers. In Figure 3 the micelle composition at different surfactant mixture compositions is plotted, assuming the interaction parameter obtained above. The predictions of the theoretical model for surfactant mixtures are valid only for low surfactant concentrations in the aqueous phase (strictly speaking, below the cmc of the anionic surfactant), but are very useful in predicting micelle formation and in the modeling of the nucleation process.

The adsorption of surfactants on the surface of particles is modeled via experimental isotherms,^{34,35} using the Langmuir isotherm:

$$\Gamma_{12} = \frac{K_{s12}C_{emul}}{1 + K_{r12}C_{emul}} \quad (43)$$

where Γ_{12} is the surface concentration of the surfactant mixture; K_{s12} and K_{r12} , the parameters of the adsorption isotherm of the mixed surfactant system; and C_{emul} , the overall emulsifier concentration.

The parameters of the adsorption isotherm are obtained from experimental parameters as follows^{36,37}:

$$K_{s12} = K_{s1}\alpha + K_{s2}(1 - \alpha) \quad (44)$$

$$K_{r12} = K_{r1}\alpha + K_{r2}(1 - \alpha) \quad (45)$$

where K_{r_i} and K_{s_i} are the parameters of the adsorption isotherm for single i emulsifier; and α , the composition of the surfactant mixture.

In this model it is supposed that the hydrophobic interactions between chains and the steric or electric repulsive interactions between polar end groups determine the area covered by the surfactant, both in the micelles and at the surface of the polymer particles. Thus the area covered by a surfactant molecule in a micelle or in a particle is considered to be the same, and the average value for the mixture is obtained as

$$a_{s12} = a_{s1}\alpha^m + a_{s2}(1 - \alpha^m) \quad (46)$$

where a_{s_i} is the area covered by a molecule of surfactant i ; and α^m , the micelle composition.

Although the micelle size has been widely studied in literature, both for anionic³⁸⁻⁴² and for non-ionic⁴³⁻⁴⁵ emulsifiers used alone, the relationship between micelle size and surfactant mixture composition has not been well reported.⁴⁶ In this model the micelle radius is obtained as

$$d_{m12} = d_{m1} + (d_{m2} - d_{m1})(1 - \alpha^m)^{1/3} \quad (47)$$

where d_{m_i} is the radius of a micelle of single emulsifier i ; and α^m , the micelle composition.

To determine whether micelles are or are not present in the aqueous phase is very important to model nucleation. The overall emulsifier in micelles is obtained as

$$E_m = (E_T - cmc_{12}V_w) - a_p N_p \frac{K_{s12}cmc_{12}}{1 + K_{r12}cmc_{12}} \geq 0 \quad (48)$$

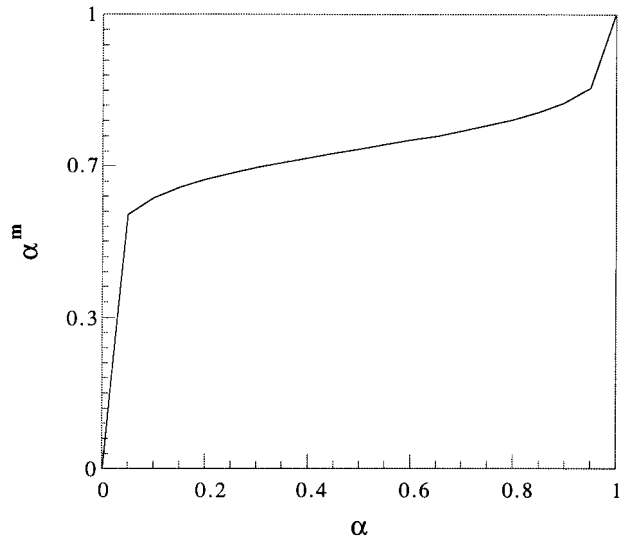


Figure 3 Composition of mixed surfactant micelles versus surfactant mixture composition.

where E_T is the total amount of emulsifier; cmc_{12} , the critical micelle concentration of surfactant mixture; and a_p , the particle area. In this expression, if $E_m > 0$, micelles are present in the aqueous phase.

If they exist, the number of micelles is obtained as

$$N_m = \frac{a_{s12} E_m}{\pi d_{m12}^2} \quad (49)$$

where a_{s12} is the average area covered by a surfactant molecule of the surfactant mixture; and d_{m12} , the radius of mixed micelles. The emulsifier amount in the aqueous phase is

$$E_w = cmc_{12} V_w \quad (50)$$

If the emulsifier concentration in the aqueous phase is below the cmc , the emulsifier in the aqueous phase is

$$E_w = \frac{-(K_{s12} a_p N_p - K_{r12} E_T + V_w) + [(K_{s12} a_p N_p - K_{r12} E_T + V_w)^2 + 4K_{r12} E_T V_w]^{1/2}}{2K_{r12}} \quad (51)$$

The parameters for nucleation used in eq. (37) are related to the micelle composition and adjustable parameters, as shown below:

$$K'_n = K'_{n2} + (K'_{n1} - K'_{n2})(\alpha^m)^{1/3} \quad (52)$$

$$K''_n = K''_{n0} - \log\left(\frac{K'_{n1}}{K'_n}\right) \quad (53)$$

where K''_{n0} , K'_{n1} , K'_{n2} , and K'_n are adjustable parameters; and α^m , the composition of mixed surfactant micelles.

Coagulation Processes

In the mathematical model developed in this work the possibility of coagulative processes between particles is considered. Coagulation in colloidal systems is theoretically described in the DLVO theory.^{47,48} This theory includes a repulsive (electrostatic) and an attractive (Van der Waals interaction) term. When the repulsive force is close to zero, particle coagulation is diffusionally controlled.⁴⁹ The usual approach is to consider the

coagulation process as a kinetic process with a kinetic coagulation constant, k_g , calculated as

$$k_g = \frac{k_{go}}{W} \quad (54)$$

where k_{go} is the diffusional coagulation rate constant or fast coagulation constant⁴⁹; and W is the stability factor of Fuchs.⁵⁰ The stability factor has been related to the coverage of particle surface by the emulsifier (ν):

$$W = K'_g \exp\{K''_g \nu^{1/2}\} \quad (55)$$

where K'_g and K''_g are adjustable parameters.

Model Parameters

In the mathematical model described above, several parameters and physicochemical constants have been used. The parameters considered as non adjustable are shown in Table I. These values were obtained from the literature or from experimental results. The rate constant for fast coagulation (k_{go}) was obtained turbidimetrically.⁵¹ The critical micelle concentrations for SLS and Brij35 were obtained from surface tension measurements at different emulsifier concentrations. The interaction parameter between both emulsifiers was also obtained from surface tension measurements, as explained above.

The adjustable parameters are shown in Table II. These parameters were chosen to fit the experimental data used as reference in this work.^{14,15}

RESULTS AND DISCUSSION

In this work we have focused our attention on the effect of mixed surfactant systems (anionic/non-ionic) on nucleation by means of the stability of the precursor particles and on the partition of surfactant between particles, micelles, and the aqueous phase. The model presented is an attempt to fit a range of different types of experimental data obtained in a previous study^{14,15} of the effect of mixed surfactant systems in the emulsion copolymerization of methyl methacrylate and butyl acrylate in a semicontinuous reactor. The model provides a pragmatic and predictive approach to fit the experimental data.

Initially, the effect of the number of moments used to obtain the PSD was studied. Figure 4

Table I Nonadjustable Parameter Values

$M_{\text{MMA}}, M_{\text{BuA}}$ (g/mol) ⁵⁵	100.12, 128.17
$\rho_{\text{pMMA}}, \rho_{\text{pBuA}}$ (g/cm ³) ⁵⁵	1.19, 1.08
$\bar{V}_{\text{MMA}}, \bar{V}_{\text{BuA}}$ (cm ³ /mol) ⁵⁵	106.62, 142.44
$M_{\text{SLS}}, M_{\text{Brij35}}$ (g/mol)	288, 1198
$K_A^d, K_A^p, K_B^d, K_B^p$ ⁵⁶	59.03, 43.09, 705.4, 458.4
$k_{\text{pAA}}, k_{\text{pBB}}$ ⁵⁷ (cc/mol s)	$9.2 \times 10^5, 2.47 \times 10^5,$
$k_{\text{pAB}}, k_{\text{pBA}}$ ¹⁹ (cc/mol s)	$3.49 \times 10^5, 7.8 \times 10^5$
$k_{\text{tAA}}, k_{\text{tBB}}, k_{\text{tAB}}, k_{\text{tBA}}$ ⁵⁵ (cc/mol s)	$1.9 \times 10^{10}, 1.6 \times 10^6, 1.7 \times 10^8, 1.7 \times 10^8$
$k_{\text{fAA}}, k_{\text{fBB}}, k_{\text{fAB}}, k_{\text{fBA}}$ ⁵⁵ (cc/mol s)	9.205, 14.65, 11.62, 11.62
D_W, D_p ¹⁸	$10^{-5}, 10^{-6}$
$a_{\text{sSLS}}, a_{\text{sBrij35}}$ ³⁶ (cm ² /mol)	$3.2 \times 10^9, 5.1 \times 10^9$
$cmc_{\text{SLS}}, cmc_{\text{Brij35}}$ (mol/cm ³)	$2.43 \times 10^{-6}, 1.1 \times 10^{-7}$
$d_{\text{mSLS}}, d_{\text{mBrij35}}$ ^{42, 43} (nm)	5, 10
k_{go} (cm ³ /part s)	3×10^{-12}
$K_{\text{sSLS}}, K_{\text{sBrij35}}$ ^{36, 37} (cm)	$2.5 \times 10^{-3}, 1.56 \times 10^{-3}$
$K_{\text{rSLS}}, K_{\text{rBrij35}}$ ^{36, 37} (cm ³ /mol)	$8 \times 10^6, 7.9 \times 10^6$
f ¹⁸	0.6
β^m	-8
r_{po}^* ²⁷ (nm)	5

shows the PSDs obtained using 6 and 14 moments of the experimental distributions, where the theoretical fit to the experimental distributions is better the greater the number of moments used. All the simulations of this work were carried out using 14 moments. Furthermore, Figure 5 demonstrates the ability of this method to fit bimodal distributions.

Model Predictions for a Batch Reactor

The effect of the emulsifier concentration (taking as reference the anionic surfactant concentration) at different mixture compositions on the particle number obtained, was simulated for a batch reactor. Simulations were carried out using the recipe shown in Table III at 70°C. In Figure 6, the particle number obtained per cubic centimeter of water versus anionic surfactant (SLS) concentration at different mixture compositions is shown (in each composition the SLS amount is the reference, while the Brij35 amount is obtained from the SLS/Brij35 ratio).

In Figure 6, the particle concentration is insen-

sitive to surfactant concentration at low and high concentrations for the run in which SLS is used alone. These results agree with previously reported experimental results.⁵²⁻⁵⁴ In this case, the particle concentration increases sharply near the *cmc*. On the other hand, when the nonionic one (Brij35) is used alone, the increase is slighter and, beginning close to the *cmc*, it extends over a wide concentration range. Moreover, the particle number obtained at high concentrations is much lower than that obtained with SLS alone.

In mixed surfactant compositions, the slope of the transition decreases (compared with SLS

Table II Adjustable Parameter Values

F_p, F_m	$10^{-4}, 10^{-5}$
k_g', k_g''	$10^4, 15$
$K_{n1}', K_{n2}', K_{n0}''$	$1.0, 10^{-3}, 12$
kg^{**}, kg^{*p} (cm ³ /part s)	$10^{-15}, 10^{-16}$

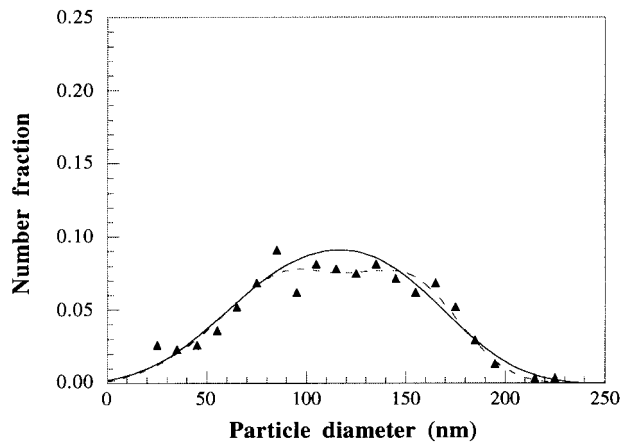


Figure 4 Effect of the number of moments used to obtain a PSD: (▲) experimental; (—) theoretical, 6 moments; (---) theoretical, 14 moments.

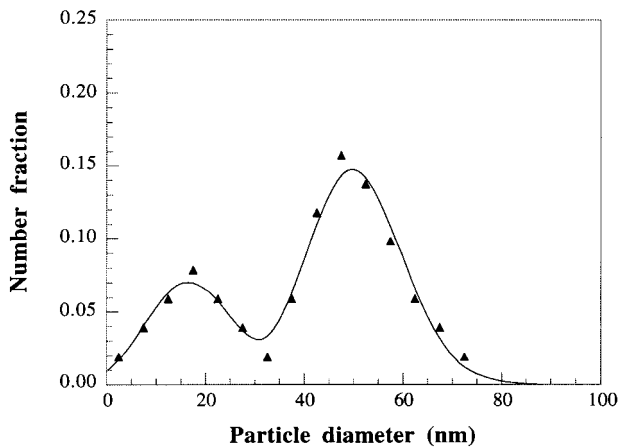


Figure 5 PSD calculated from a bimodal distribution: (▲) experimental; (—) theoretical, 14 moments.

alone) and it starts at lower concentrations. This is due to the *cmc* of the mixture being much lower than the *cmc* of the SLS alone (see Fig. 2). On the other hand, at high emulsifier concentrations, the particle number obtained is close to that obtained with SLS alone. The behavior at low concentrations is determined by the nonionic surfactant (decreasing the *cmc* of the mixture) but, at higher concentrations, the anionic one determines the particle number obtained.

Model Predictions for a Semicontinuous Reactor

The experimental results reported in a previous paper¹⁴ were compared with theoretical results obtained with this model. Simulated runs are non-seeded emulsion copolymerization reactions carried out in semicontinuous reactor. To simulate the actual experimental conditions, the initial inhibition time measured in each experimental run (while the monomer feeding is started) was included as a new adjustable parameter.

Table III Recipe Used in Batch Simulations

Compound	Weight (g)
Water	100
MMA	14.1
BuA	18
K ₂ S ₂ O ₈	0.126
SLS	Variable
Brij35	Variable

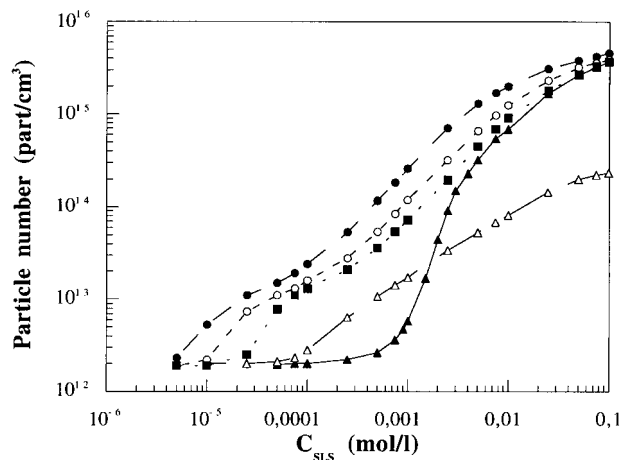


Figure 6 Effect of surfactant concentration at different mixture compositions on the particle number in a batch reactor. SLS/Brij35 mole fraction: (▲) 1/0; (■) 75/25; (○) 50/50; (●) 25/75; (△) 0/1.

Figure 7 shows the effect of the emulsifier mixture composition on the evolution of the instantaneous conversion for experimental runs and for model predictions. In the chosen reactions the initial amount of SLS (or Brij35 in the nonionic single system) was 1.25 g and the amount of Brij35 in mixtures was proportional to the desired sur-

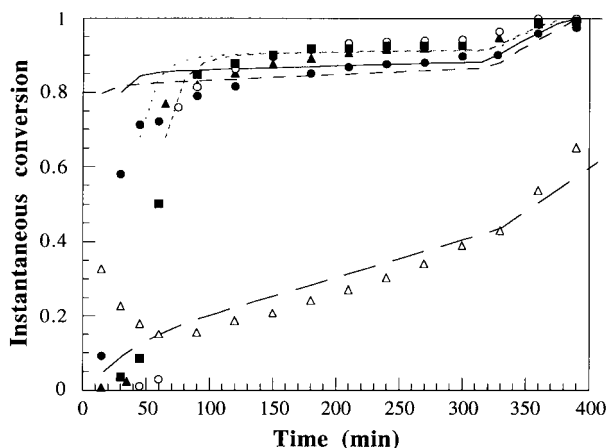


Figure 7 Effect of surfactant mixture composition on the evolution of the instantaneous conversion in a semicontinuous reactor.

Run	SLS/Brij35	Experimental	Model
E27	1/0	▲	—
E32	0/1	△	—
E34	1/1	●	----
E37	1/3	○	----
E38	1/9	■

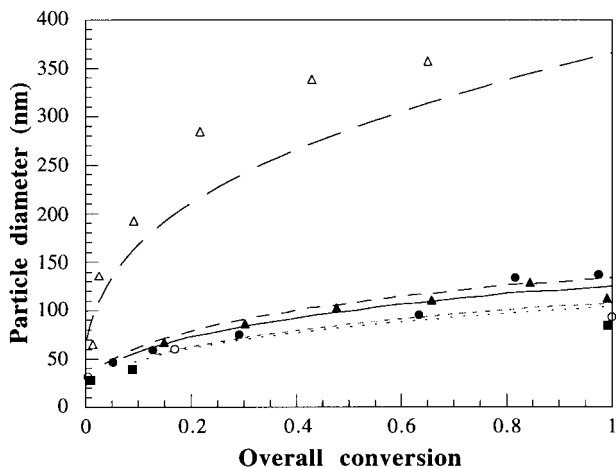


Figure 8 Effect of surfactant mixture composition on particle size evolution in a semicontinuous reactor.

Run	SLS/Brij35	Experimental	Model
E27	1/0	▲	—————
E32	0/1	△	—————
E34	1/1	●	-----
E37	1/3	○
E38	1/9	■

factant mixture composition. A good agreement between experimental and theoretical results is obtained. The mathematical model predicts that the use of a non-ionic single system does not allow the achievement of starved conditions, as found experimentally.

In Figures 8 and 9, the effect of the emulsifier mixture composition on the evolution of the volume average diameter of polymer particles and overall particle number for the same experimental runs and for the corresponding model predictions is shown. In Figure 8, when the non-ionic emulsifier is used alone, the particle diameters obtained are much larger during the entire reaction. On the other hand, the mathematical model predicts that the particle diameters found are larger when the used surfactant ratio (SLS/Brij35) is 1/1 than when it is 1/0 (single anionic emulsifier), although the overall surfactant concentration is higher in the first case. This result was found experimentally. In Figure 9, both the experimental and the theoretical overall particle numbers are constant during the reaction, indicating that at these conditions the particles present in the reactor are born in a short nucleation process at the beginning of the run.

In emulsion copolymerization, the composition of the obtained copolymer is a primordial product quality requirement. Figure 10 shows the effect of the emulsifier mixture composition on the copolymer composition obtained for experimental runs and theoretical predictions, and a very good agreement between them is found.

In Figures 7 to 10, the effect of surfactant mixture composition on the evolution of instantaneous conversion, volume average diameter of particles, total particle number, and copolymer cumulative composition is shown. In all cases, the agreement between experimental and predicted values is good.

Figures 11 and 12 show the effect of surfactant concentration (referred to the initial anionic surfactant concentration) on the evolution of the volume average diameter of polymer particles and overall particle number for experimental runs and for their corresponding model predictions. In both figures a good agreement between the experimental and theoretical results was obtained over a wide diameter range and for particle numbers differing by two orders of magnitude. These results, compared with those mentioned above, indicate that the average particle diameters and corre-

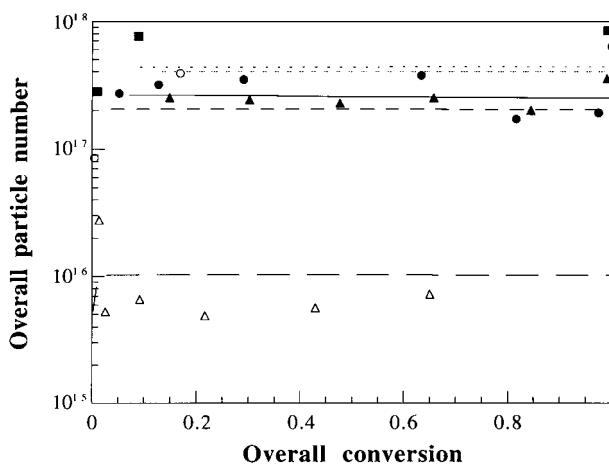


Figure 9 Effect of surfactant mixture composition on the overall particle number evolution in a semicontinuous reactor.

Run	SLS/Brij35	Experimental	Model
E27	1/0	▲	—————
E32	0/1	△	—————
E34	1/1	●	-----
E37	1/3	○
E38	1/9	■

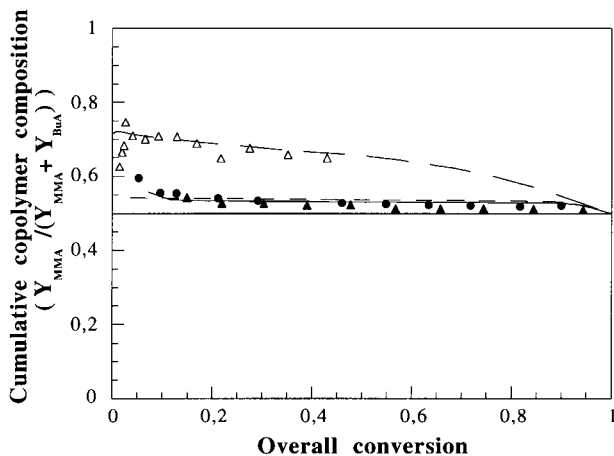


Figure 10 Effect of surfactant mixture composition on the cumulative copolymer composition in a semicontinuous reactor.

Run	SLS/Brij35	Experimental	Model
E27	1/0	▲	—————
E32	0/1	△	—————
E34	1/1	●	- - - - -

sponding particle numbers are more sensitive to surfactant concentration changes than to mixture composition changes.

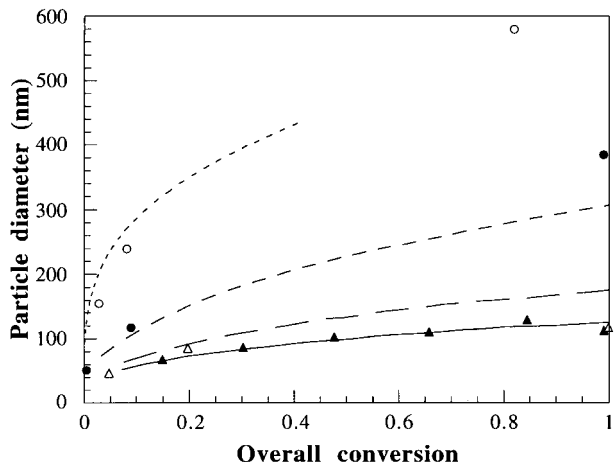


Figure 11 Effect of surfactant concentration on particle size evolution in a semicontinuous reactor.

Run	C_{SLS_0} (g)	Experimental	Model
E27	1.125	▲	—————
E39	0.388	△	—————
E44	0.097	●	- - - - -
E49	0.039	○	- - - - -

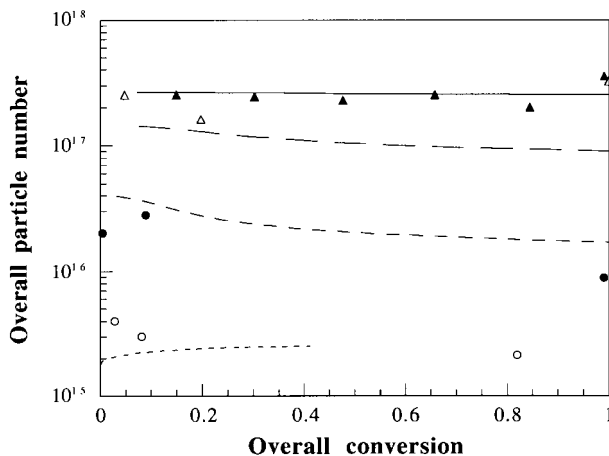


Figure 12 Effect of surfactant concentration on particle number evolution in a semicontinuous reactor.

Run	C_{SLS_0} (g)	Experimental	Model
E27	1.125	▲	—————
E39	0.388	△	—————
E44	0.097	●	- - - - -
E49	0.039	○	- - - - -

CONCLUSIONS

A mathematical model for emulsion polymerization has been developed, using the method of moments to simulate the evolution of the particle size distribution, and applicable in batch or semicontinuous reactors. The model is a set of differential equations of material balances and population balances of the precursor particles and the moments of the particle size distribution.

This model predicts the evolution of conversion, copolymer composition, particle average diameters, and particle numbers during the reaction. The model is sensitive both to the surfactant concentration and to surfactant mixture composition (anionic/nonionic). A good agreement between predictions and experimental data was achieved.

A nucleation model based on competition between homogeneous and heterogeneous nucleation has been developed, combined with the assumptions of the coagulative nucleation theory.

Using the thermodynamics of nonideal mixtures, the solution properties of surfactant mixtures were calculated, mainly critical micellar concentration and micelle composition.

This work is supported by the Comision Interministerial de Ciencia y Tecnología (CICYT), project MAT96-1035-C03-01, and by the Gipuzkoako Foru Aldundia.

NOMENCLATURE

α_s	surfactant specific area ($\text{cm}^2 \text{mol}^{-1}$)	N_A	Avogadro's constant (molecules mol^{-1})
cmc_i	critical micelle concentration of surfactant i (mol L^{-1})	N_m	total micelle number
d_m	micelle diameter (nm)	N_p	total particle number
\bar{d}_a	area average diameter (nm)	N^*	number of precursor particles
\bar{d}_n	number average diameter (nm)	P_i^j	propagation probability of an i radical in phase j
\bar{d}_v	volume average diameter (nm)	P_N	probability of a precursor particle to become a mature particle
\bar{d}_w	weight average diameter (nm)	PSD	particle size distribution
D_p	radical diffusion constant in particles ($\text{cm}^2 \text{s}^{-1}$)	Q_w	water volumetric feed rate ($\text{cm}^3 \text{s}^{-1}$)
D_w	radical diffusion constant in aqueous phase ($\text{cm}^2 \text{s}^{-1}$)	r	particle radius (nm)
E_i	overall amount of surfactant i (mol)	r_m	micelle radius (nm)
E_m	surfactant amount in micelles (mol)	r_p	particle radius (nm)
E_T	overall amount of surfactant (mol)	r_{po}	critical radius for mature particles (nm)
E_w	surfactant amount in aqueous phase (mol)	r_{po}^*	initial radius for precursor particles (nm)
f	initiator decomposition efficiency	R_h	fraction of homogeneous nucleation
F_i	molar feed rate of i (mol s^{-1})	R_m	fraction of micellar nucleation
F_m	absorption efficiency to micelles	R_g	nucleation rate for precursor particles (s^{-1})
F_p	absorption efficiency to particles	R_w	radical concentration in aqueous phase (mol cm^{-3})
g^2	gel effect parameter	v_p	particle volume (cm^3)
j_{cr}	critical radical chain length	\bar{v}_i	molar volume of i ($\text{cm}^3 \text{mol}^{-1}$)
k_a	absorption rate constant to particles ($\text{cm}^3 \text{mol}^{-1} \text{s}^{-1}$)	V_w	water volume (cm^3)
k_{am}	absorption rate constant to micelles ($\text{cm}^3 \text{mol}^{-1} \text{s}^{-1}$)	W	stability factor of Fusch
k_d	desorption rate constant (s^{-1})	x_p	conversion in particles
k_g	coagulation rate constant ($\text{cm}^3 \text{part}^{-1} \text{s}^{-1}$)	α	composition of surfactant mixture
k'_g	coagulation adjustable parameter	α^m	composition of mixed surfactant micelles
k''_g	coagulation adjustable parameter	β^m	surfactant interaction parameter
k_{go}	rapid coagulation rate constant ($\text{cm}^3 \text{part}^{-1} \text{s}^{-1}$)	Γ	surfactant surface concentration (mol cm^{-2})
k_g^{**}	coagulation rate constant between precursor particles ($\text{cm}^3 \text{part}^{-1} \text{s}^{-1}$)	μ^i	moment of i th order (nm^i) of the PSD
k_g^{*p}	coagulation rate constant between precursor and mature particles ($\text{cm}^3 \text{part}^{-1} \text{s}^{-1}$)	ρ	density (g cm^{-3})
K_i^j	partition constant of monomer i in phase j	ρ_I	radical generation rate from initiator (s^{-1})
k_I	initiator decomposition rate constant (s^{-1})		
k_{fij}	transfer rate constant between monomer units i and j ($\text{cm}^3 \text{mol}^{-1} \text{s}^{-1}$)		
k_{pij}	propagation rate constant between monomer i and j ($\text{cm}^3 \text{mol}^{-1} \text{s}^{-1}$)		
k_{tij}	termination rate constant between monomer i and j ($\text{cm}^3 \text{mol}^{-1} \text{s}^{-1}$)		
K_s	constant for adsorption isotherm (cm)		
K_r	constant for adsorption isotherm ($\text{cm}^3 \text{mol}^{-1}$)		
K'_n	adjustable parameter for nucleation		
K''_n	adjustable parameter for nucleation		
M_i	molecular weight of i (g mol^{-1})		
\bar{n}	average radical number per particle		

REFERENCES

1. E. D. Sudol, E. S. Daniels, and M. S. El-Aasser, *ACS Symp. Ser.*, **492**, 1 (1992).
2. W. D. Harkins, *J. Am. Chem. Soc.*, **69**, 1428 (1947).
3. W. V. Smith and R. H. Ewart, *J. Chem. Phys.*, **16**, 592 (1948).
4. B. Li and B. W. Brooks, *J. Appl. Polym. Sci.*, **48**, 1811 (1993).
5. J. Forcada and J. M. Asua, *J. Polym. Sci., Part A: Polym. Chem. Ed.*, **29**, 1231 (1991).
6. J. Guillet, *Makromol. Chem., Macromol. Symp.*, **35/36**, 269 (1990).
7. G. Lichti, R. G. Gilbert, and D. H. Napper, *J. Polym. Sci.: Polym. Chem. Ed.*, **21**, 269 (1983).
8. G. Arzamendi and J. M. Asua, *J. Appl. Polym. Sci.*, **38**, 2019 (1989).
9. B. Urquiola, G. Arzamendi, J. R. Leiza, A. Zamora, J. M. Asua, J. Delgado, M. S. El-Aasser, and J. W. Vanderhoff, *J. Polym. Sci., Part A: Polym. Chem.*, **29**, 169 (1991).

10. G. Arzamendi and J. M. Asua, *Ind. Eng. Chem. Res.*, **30**, 1342 (1991).
11. G. Arzamendi and J. M. Asua, *Makromol. Chem., Macromol. Symp.*, **35/36**, 249 (1990).
12. F. K. Hansen and J. Ugelstad, in *Emulsion Polymerization*, I. Piirma, Ed., Academic Press, New York, 1982.
13. R. M. Fitch and C. H. Tsai, in *Polymer Colloids I*, R. M. Fitch, Ed., Plenum Press, New York, 1971.
14. E. Unzueta and J. Forcada, *Polymer*, **36**(5), 1045 (1995).
15. E. Unzueta and J. Forcada, *Polymer*, **36**(22), 4301 (1995).
16. C. W. Gear, in *IMSL Math / Library*, IMSL Inc., Houston, 1990.
17. K. W. Min, Ph.D. thesis, State University of New York at Buffalo, 1976.
18. J. Forcada and J. M. Asua, *J. Polym. Sci., Part A: Polym. Chem., Ed.*, **28**, 987 (1990).
19. A. Urretabizkaia, Ph.D. thesis, Universidad del País Vasco and Euskal Herriko Unibertsitatea, 1993.
20. S. Omi, K. Kushibiki, M. Negishi, and M. Iso, *Zairyo Gijutsu*, **3**(9), 426 (1985).
21. J. Ugelstad and F. K. Hansen, *Rubber Chem. Technol.*, **49**, 536 (1976).
22. R. M. Fitch and L. B. Shih, *Progr. Colloid Polym. Sci.*, **56**, 1 (1975).
23. J. M. Asua, E. D. Sudol, and M. S. El-Aasser, *J. Polym. Sci., Part A: Polym. Chem. Ed.*, **27**, 3903 (1989).
24. F. L. Marten and A. E. Hamielec, *ACS Symp. Ser.*, **104**, 43 (1979).
25. F. K. Hansen, *Chem. Eng. Sci.*, **48**(2), 437 (1993).
26. F. K. Hansen and J. Ugelstad, *J. Polym. Sci., Polym. Chem. Ed.*, **16**, 1953 (1978).
27. W. Hergeth, W. Lebek, E. Stettin, K. Witkowski, and K. Schmutzler, *Makromol. Chem.*, **193**, 1607 (1992).
28. M. J. Rosen, in *Surfactants and Interfacial Phenomena*, John Wiley & Sons, New York, 1989.
29. M. J. Rosen and X. Y. Hua, *J. Colloid Interface Sci.*, **86**(1), 164 (1982).
30. M. J. Rosen and F. Zhao, *J. Colloid Interface Sci.*, **95**(2), 443 (1983).
31. M. J. Rosen and B. Y. Zhu, *J. Colloid Interface Sci.*, **99**(2), 427 (1984).
32. M. J. Rosen and D. S. Murphy, *J. Colloid Interface Sci.*, **110**(1), 224 (1986).
33. M. J. Rosen and B. Gu, *Colloids and Surfaces*, **23**, 119 (1987).
34. B. Y. Zhu and T. Gu, *J. Chem. Soc., Faraday Trans. 1*, **85**(11), 3813 (1989).
35. B. Y. Zhu, T. Gu, and X. Zhao, *J. Chem. Soc., Faraday Trans. 1*, **85**(11), 3819 (1989).
36. J. G. Brodnyan and E. L. Kelley, *J. Polym. Sci., Part C*, **27**, 263 (1969).
37. A. Martín, Ph.D. thesis, Universidad de Granada, 1993.
38. P. J. Missel, N. A. Mazer, G. B. Benedek, and M. C. Carey, *J. Phys. Chem.*, **87**, 1264 (1983).
39. P. J. Missel, N. A. Mazer, G. B. Benedek, and C. Y. Young, *J. Phys. Chem.*, **84**, 1044 (1980).
40. J. Briggs, D. F. Nicoli, and R. Ciccolello, *Chem. Phys. Lett.*, **73**(1), 149 (1980).
41. A. Rohde and E. Sackmann, *J. Colloid Interface Sci.*, **70**(3), 494 (1979).
42. N. A. Mazer and G. B. Benedek, *J. Phys. Chem.*, **80**(10), 1075 (1976).
43. M. Corti and V. Degiorgio, *Optics Commun.*, **14**(3), 358 (1975).
44. D. J. Cebula and R. H. Ottewill, *Colloid Polym. Sci.*, **260**, 1118 (1982).
45. P. G. Nilsson, H. Wennerström, and B. Lindman, *J. Phys. Chem.*, **87**, 1377 (1983).
46. I. Piirma and P. Wang, *ACS Symp. Ser.*, **24**, 34 (1976).
47. B. V. Derjaguin and L. Landau, *Acta Physicochimica URSS*, **14**, 633 (1941).
48. E. J. W. Verwey and J. T. G. Overbeek, in *Theory of the Stability of Lyophobic Colloids*, Elsevier, Amsterdam, 1948.
49. M. V. Smoluchowski, *Z. Phys.*, **17**, 557 (1917).
50. N. Fuchs, *Z. Phys.*, **89**, 736 (1934).
51. J. W. T. Lichtenbelt, H. J. M. C. Ras, and P. H. Wiersema, *J. Colloid Interface Sci.*, **46**(3), 522 (1974).
52. B. M. E. v. d. Hoff, *J. Polym. Sci.*, **48**, 175 (1960).
53. S. Okamura and T. Motoyama, *J. Polym. Sci.*, **58**, 221 (1962).
54. A. S. Dunn, in *Polymer Colloids II*, R. M. Fitch, Ed., Plenum Press, New York, 1980.
55. J. Brandrup and E. H. Immergut, Eds., *Polymer Handbook*, Wiley-Interscience, New York, 1989.
56. J. Delgado, Ph.D. thesis, Lehigh University, Bethlehem, PA, 1986.
57. C. Walling, *Free Radicals in Solution*, Wiley-Interscience, New York, 1976.